

X-Ray diffraction and magnetization study of $\text{Ni}_{0.5}\text{Cu}_{0.3}\text{Zn}_{0.2}\text{Cr}_x\text{Fe}_{2-x}\text{O}_4$ ferrite nano particles synthesized by Sol-gel method

Pallavi S. Salunke¹ and Suresh T. Alone^{1*}

¹Department of Physics, Rajarshi Shahu A. C. S. College Pathri, Tq. Phulambri, Dist. Aurangabad. 431111

*Corresponding Author:

Abstract: $\text{Ni}_{0.5}\text{Cu}_{0.3}\text{Zn}_{0.2}\text{Cr}_x\text{Fe}_{2-x}\text{O}_4$ ($x = 0.0, 0.25, 0.50, 0.75, 1.0$) nano particles have been designed by the sol-gel auto combustion method, using nitrates of the respective metal ions, and citric acid as the starting materials. The process takes only a few minutes to obtain as-received Cr-substituted Ni-Cu-Zn ferrite powders. The X-ray analysis showed that all the samples possess single-phase cubic spinel structure. The variation of lattice constant with Ni, Zn and Cr concentration deviates from Vegard's law. Lattice parameter, particle size found to decrease within creasing Cr^{3+} content, whereas specific surface area showed increasing trend with the Cr^{3+} substitution. Particle size is obtained in nanometer scale which is obtained from XRD data. The saturation magnetization σ_s and magneton number $n_B(\mu_B)$ measured at 300 K using high field hysteresis loop technique. It is observed that saturation magnetization σ_s and magneton number $n_B(\mu_B)$ decreases with increasing the composition of x . The significant canting exists on B site suggesting magnetic structure to be non-collinear.

Keywords: Sol-Gel method; XRD, Magnetization, Nano ferrite.

INTRODUCTION:

The synthesis of their nano particles at low temperature by various methods in view of the potential applications of these nano size magnetic materials in different technological areas [1,2]. Synthesis and application of magnetic nano particles is subject of interest of several researchers because of their unique properties that makes them attractive and interesting from scientific view and technological significance of enhancing the performance of the existing materials [3, 4]. The nano-size materials exhibit unusual physical and chemical properties significantly different from those of their bulk counter part because of their extremely small size and large specific area [5,6]. Nano-size ferrites with uniform particles size and narrow size distribution are desirable for a variety of applications viz. magnetic data storage ferro-fluids, medical imaging, drug delivery etc. [7, 8], so their synthesis and characterization have attracted increasing attention in the last five years. The ability to produce nano size magnetic materials has opened new applications for magnetic materials. Keeping in view the above facts, it is decided to investigate the structural and magnetic properties of fine particle ferrites prepared by Sol-Gel method.

Ferrites continued to be very attractive materials for technological applications due to their unique electrical and magnetic properties. Ni-Zn and Mg-Zn ferrites core are found to be increasing importance in the transformer and telecommunication field as they offer inexpensive alternatives to many other soft magnetic materials. Ni-Zn ferrites are adequate for use in the high frequency band because of their high resistivity with sufficient low losses for microwave applications [9, 10]. Magnetic nanoparticles of spinel ferrites are of great interest in fundamental science, especially for addressing the fundamental relationships between magnetic properties and their crystal chemistry and structure. Superparamagnetic is a unique feature of magnetic nanoparticles and is crucially related to many modern technologies including ferrofluid technology [11], magnetocaloric refrigeration [12], contrast enhancement in magnetic resonance imaging (MRI) [13], and magnetically guided drug delivery [14]. Superparamagnetic properties have been extensively studied in the pure metal nanoparticles, such as Fe, Co, and Ni with the size confined within only a few nanometers [15–18], whose applications are limited by the poor chemical stability. Recently, more attention has been focused on the preparation and characterization of superparamagnetic metal oxide nanoparticles such as spinel ferrites, MFe_2O_4 ($M = \text{Co}, \text{Mg}, \text{Mn}, \text{Zn}, \text{etc.}$) [19–20]. Fine magnetic particle systems have been receiving a growing interest in last few years because of their wide application potentialities in the domain of nanostructured material technologies. Due to many interesting properties of fine magnetic particles, spanning from superparamagnetic to ferromagnetic, it is essential to know the properties of fine particles to be explored for a particular

application. Few such applications of nanostructured materials are magnetic recording media, magnetic fluids, catalysis, medical diagnostics, drug delivery systems, pigments in paints and ceramics.

- **To study the structural characterization by X-ray diffraction technique:**

To confirm the formation of single-phase cubic spinel structure of the newly prepared ferrite system, the X-ray diffraction patterns of all the samples were collected. The XRD patterns were used to study the structural parameters like lattice parameter, X-ray density, Cation distribution and Particle size.

- **To study the magnetic properties such as**

The magnetic measurements viz. magnetizations were carried out using pulse field hysteresis loop tracer (Magneta Company), applying 50Hz frequency. The a.c. susceptibility double coil set up operating at a frequency of 263Hz and in r.m.s. field of 100 Oe was used to record temperature variation susceptibility. The susceptibility and magnetization apparatus were calibrated with nickel prior to the measurements.

EXPERIMENTAL:

The samples of the series $\text{Ni}_{0.5}\text{Cu}_{0.3}\text{Zn}_{0.2}\text{Cr}_x\text{Fe}_{2-x}\text{O}_4$ ($x = 0.0, 0.25, 0.50, 0.75, 1.0$) are prepared by using Sol-Gel auto combustion method. The starting samples were taken in the form of Nitrates as, Nickel Nitrate, Copper Nitrate, Zinc Nitrate, and Ferric Nitrate. The obtained powder was then subjected to further heating treatment into a muffle furnace at 600°C for six hours. The final product is then grinded and subjected to further study. X-ray diffractions of all the prepared samples was taken in the 2θ range of 20 degree to 80 degree in the step of 2 degree/minute at room temperature. After confirmation of the structure of all the samples, the powders are then converted in to the pellet form having dimensions 10 mm diameter and 2-3 mm thickness. The pellets were then used to study the electrical properties. Two probe techniques were used to study the magnetic properties like magnetization. The temperature for this study is varying from 300 K to 800K.

RESULTS AND DISCUSSION:

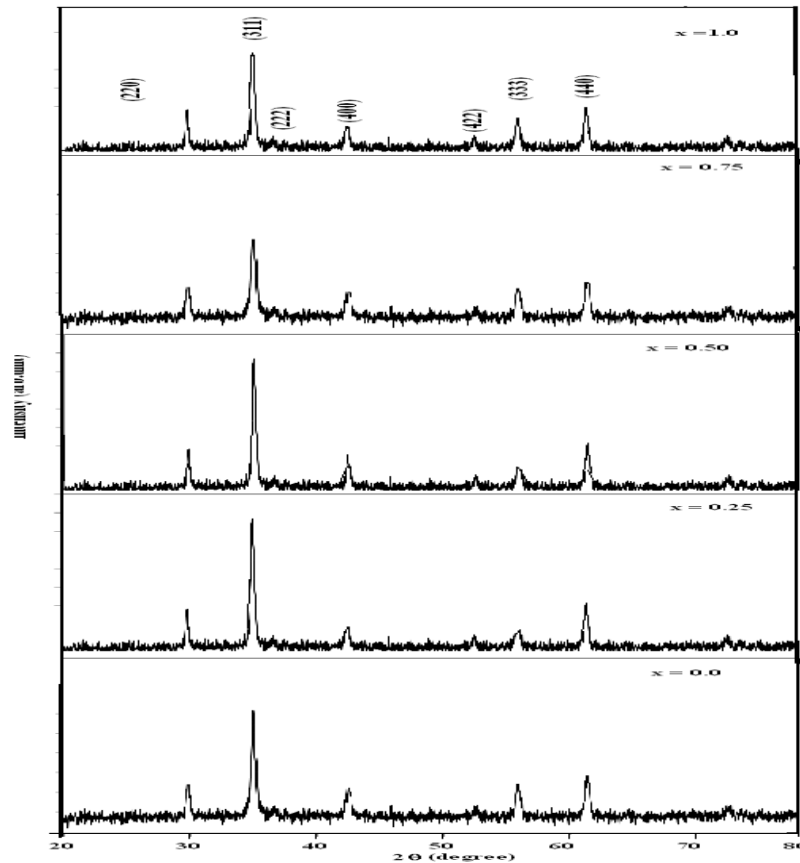


Fig 1: X-ray diffraction patterns of samples for the system $\text{Ni}_{0.5}\text{Cu}_{0.3}\text{Zn}_{0.2}\text{Cr}_x\text{Fe}_{2-x}\text{O}_4$ ($x = 0.0, 0.25, 0.50, 0.75, 1.0$)

Figure 1 shows the X-ray diffraction patterns of the series $\text{Ni}_{0.5}\text{Cu}_{0.3}\text{Zn}_{0.2}\text{Cr}_x\text{Fe}_{2-x}\text{O}_4$ ($x = 0.0, 0.25, 0.50, 0.75, 1.0$) prepared by sol-gel auto-combustion technique. The XRD peak shows sharp Bragg's peaks and there is no any impurity peak observed. All the peaks are indexed by miller indices and it reveals that all the sample possess the single-phase cubic spinel structure. The structural parameters like lattice parameter 'a', Particle size 't' and X-ray density 'd_x' was calculated from the data obtained from X-ray diffraction patterns. The variation of lattice parameter 'a' with composition 'x'. It is observed that the lattice parameter decreases with increase in Cr content 'x'. It is due to the replacement of smaller ionic radii atom Fe (0.645 A.U.) is replaced by smaller ionic radii of Chromium (0.615 A.U.). The particle size of all the samples was obtained in the range 20 nm to 28 nm. Lattice constant, X ray density and particle size for the system $\text{Ni}_{0.5}\text{Cu}_{0.3}\text{Zn}_{0.2}\text{Cr}_x\text{Fe}_{2-x}\text{O}_4$ which is listed in Table 01.

The XRD line width and particle size are connected to Scherrer equation,

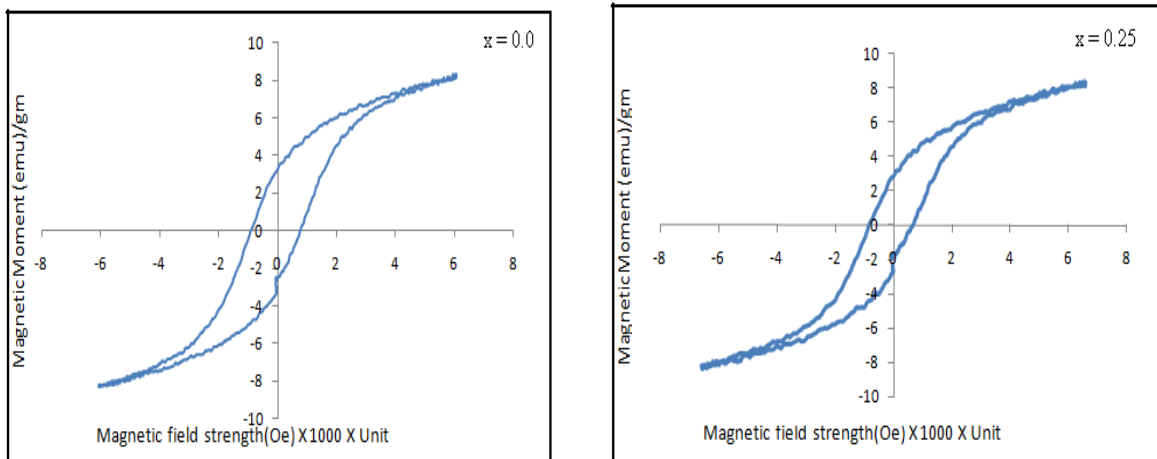
$$t = \frac{0.9\lambda}{B \cos\theta_B}, \text{ with } B^2 = B_a^2 - B_b^2 \tag{1}$$

where, t is diameter of crystal particle, λ is wavelength of the X-ray radiation, θ_B is Bragg's angle, B is measure of broadening of diffraction due to size effect B_a and B_b are full width at half maxima of the XRD line of the sample and standard specimen respectively.

Table1: Lattice constant, X ray density and particle size for the system $\text{Ni}_{0.5}\text{Cu}_{0.3}\text{Zn}_{0.2}\text{Cr}_x\text{Fe}_{2-x}\text{O}_4$

x	Lattice Constant a (A°)	X-ray density d _x	Particle size t
0.0	8.331	5.460	20
0.25	8.317	5.474	23
0.50	8.302	5.482	25
0.75	8.277	5.491	27
1.0	8.257	5.507	28

Figure 2 shows the variation of Magnetic field strength (B) with Magnetic moment. From the graph it is observed that the Magnetic field strength (B) with Magnetic moment decreases for all the samples of the present series.



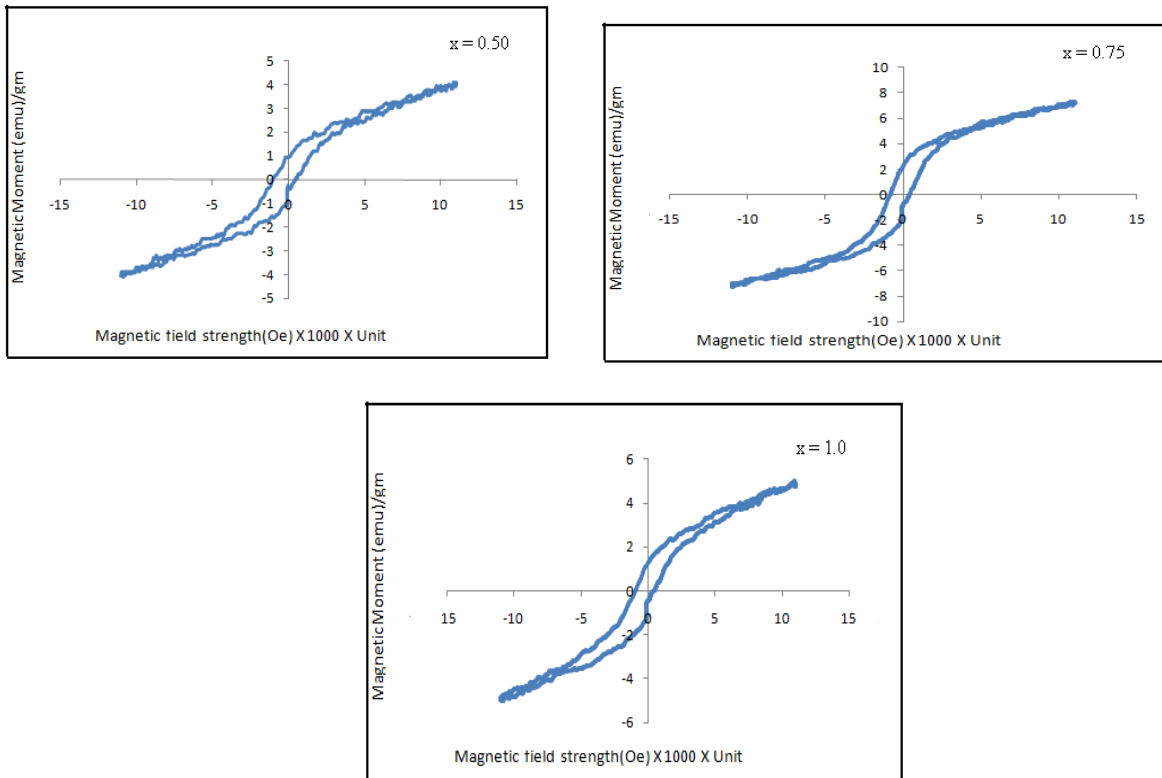


Fig. 2. Variation of Magnetic field strength (B) with Magnetic moment of samples for the system $\text{Ni}_{0.5}\text{Cu}_{0.3}\text{Zn}_{0.2}\text{Cr}_x\text{Fe}_{2-x}\text{O}_4$ ($x = 0.0$ to $0.25, 5.0, 7.5, 1.0$)

The saturation magnetization (σ_s) and the magneton number (n_B) The saturation magnetization per formula unit in Bohr magneton at 300 K were obtained from magnetization data for the samples $x = 0.0$ to $x = 1.0$ and same is summarized in Table 2. It is seen that the values of n_B^C (μ_B) gradually decreases with increase in 'x' suggesting decrease in ferrimagnetism. The values calculated using Neels collinear model n_B^N (μ_B) and cation distribution are also represented in Table 2. These calculated values differ with the experimentally determined values suggesting canted structure. This canting exists on [B] site $[\text{Cu}_{0.6}\text{Cr}_x\text{Fe}_{2-x}]$ due to nonmagnetic substitution of Cr suggesting the magnetic structure to be non collinear [21]. The values calculated using Neels collinear model n_B^N (μ_B) and observed values are in good agreement shown in Fig 3.

The data suggest that the canting is not uniform but instead it is locally dependent upon statistical distribution of nonmagnetic neighbouring ions. Therefore, the increase in Cr^{3+} substitution leads to localized non collinearity of the ferrimagnetic structure by local canting around the magnetic imperfections introduced by Cr- substitution. It is evident from the cation distribution formula that the difference in the fraction of Fe^{3+} ions on B-site and A-site $|\text{C}_B - \text{C}_A|$ decreases linearly for the range studied. which is listed in Table 02.

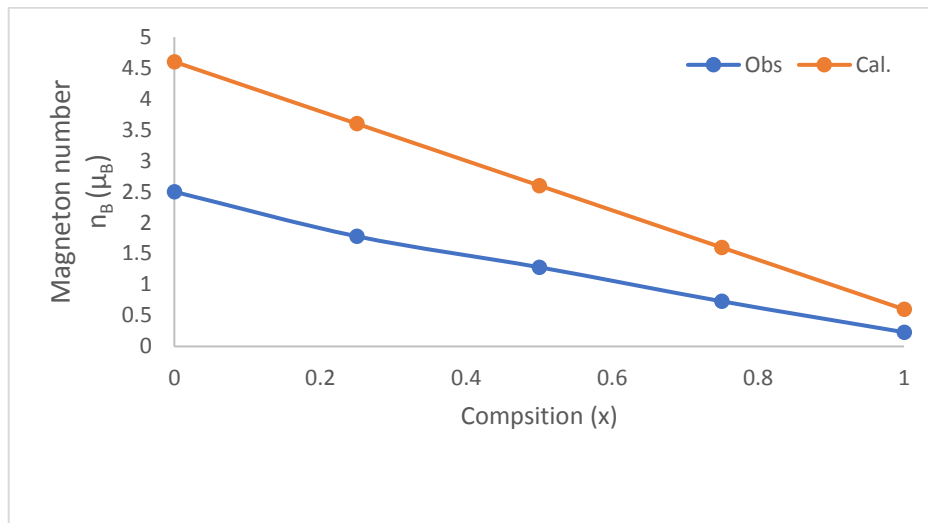


Fig. 3 Variation of observed and calculated magneton number n_B (μ_B) for the system $Ni_{0.5}Cu_{0.3}Zn_{0.2}Cr_xFe_{2-x}O_4$ ($x = 0.0, 0.25, 0.50, 0.75, 1.0$)

Table 2: Saturation magnetization (σ_s), magneton number n_B (μ_B), difference of Fe ions on B-site and A-site $|C_B - C_A|$ and canting angle θ_B for the system $Ni_{0.5}Cu_{0.3}Zn_{0.2}Cr_xFe_{2-x}O_4$

x	Saturation magnetization σ_s (emu/g)	Magneton number n_B (μ_B)		$ C_B - C_A $	θ_B (degree)
		Obs.	Cal.		
0.0	58.29	2.50	4.60	0.8	43.64
0.25	42.58	1.78	3.60	0.6	43.59
0.50	31.32	1.28	2.60	0.4	40.15
0.75	18.41	0.73	1.60	0.2	35.73
1.0	05.93	0.23	0.60	0.0	26.20

The values of n_B^N are determined using the Neels two sublattice model [22] as

$$n_B^N = m_B(x) - m_A(x) \tag{2}$$

where m_A and m_B are the (A) and [B] sub-lattice magnetic moments in (μ_B). The cation distribution is used to determine the m_A and m_B with Fe^{3+} ($5 \mu_B$), Cu^{2+} ($1\mu_B$), Cr^{3+} ($0\mu_B$) and Zn^{3+} ($0\mu_B$). The canting angle θ_B can be determined from the random canting model [23] as

$$n_B^C = m_B \cos\theta_B + m_A \quad \text{and} \quad \theta_B = \cos^{-1}[(n_B^C - m_A) / m_B] \tag{3}$$

The values of θ_B are represented in Table 2. Further it has been observed that the experimental data for the case of $x=1.0$ is $n_B^C=0.0$ suggesting the ferrimagnetism in the sample at 300K. The canting angle decreases with increase in Cr^{3+} concentration.

CONCLUSION:

Nanocrystalline Cr^{3+} substitution into the Ni-Cu-Zn was successfully prepared using sol-gel auto-combustion technique. It is observed that the lattice parameter decreases with the Cr^{3+} doping, which is explained on the basis of the smaller ionic radii of the Cr^{3+} ion than the Fe^{3+} ion. The formations of samples are confirmed that the sample possesses the single-phase cubic spinel structure of the newly prepared ferrite system. The magnetization studies suggest that the structure is to be non collinear which leads to develop the canted spin structure. The canting exists on [B] sub-lattice diluting Fe^{3+} concentration by nonmagnetic Cr^{3+} shows canting angle decreases with composition x .

REFERENCES

- [1] M. Tsuji, T. Kodama, Yoshida, V. Kitayama, Y. Tamaura, *J. Catalysis* 164 (1996) 315.
- [2] X. Yi, Q. Yital, L. Jing, C. Zuyao, Y. Li., *Mater. Sci. Eng. B34* (1995) 1.
- [3] R. Skmoski *J. Phys :Condens, Matter* 15 (2003) R841.
- [4] M.R.J. Gibbs, *Curr. Opin. Solid State Material Sci.* 7 (2003) 83.
- [5] R. J. Willey, P. Noirclerc, G. Busca, *Chem. Eng. Commun.* 123 (1993) 1.
- [6] A. T. Raghavender, Damir Pajic, Kreso Zadro, Tomislav Milekovic, P. Venkatwshwar Rao, K. M. Jadhav, D. Ravinder, *J. Magn. Magn. Mater.* 316 (2007) 1.
- [7] G. Busca, E. Finocchio, V. Lorenzelli, M. Trombetta, S. A. Rossini, *J. Chem. Soc., Faraday Trans.* 92 (1996) 4687.
- [8] Y. Shimizu, H. Arai, T. Seiyama, *Sens. Actuators* 7 (1985) 3156.
- [9] Kyung Young Kim, Jongkyu Lee, Wangsup Kim and Hwan Choi, *J. Korean Inst. Telematics and Electronics*, 28A (11) (1991) 880
- [10] S. Nishigaki, S. Yano, H. Kato, T. Nano-mora, *J. Am. Ceram. Soc.* 71 (1) C-11-0-17 (1988)
- [11] K. Raj, R. Moskowitz, R. Casciari, *J. Magn. Magn. Mater.* 149 (1995) 174.
- [12] R. D. McMichael, R. D. Shull, L. J. Swartzendruber, L. H. Bennett, *J. Magn. Magn. Mater.* 111 (1992) 29.
- [13] D. G. Mitchell, *J. Magn. Reson. Imaging* 7 (1997) 1.
- [14] U. Häfeli, W. Schütt, J. Teller, M. Zborowski, eds. *Scientific and Clinical Applications of Magnetic Carriers*, Plenum, New York (1997).
- [15] S. Yatsuya, T. Hayashi, H. Akoh, E. Nakamura, T. Akira, *Japan J. Appl. Phys.* 17 (1978) 355.
- [16] R. B. Goldfarb and C. E. Patton, *Phys. Rev. B* 24 (1981) 1360.
- [17] S. K. Khanna and S. Linderoth, *Phys. Rev. Lett.* 67 (1991) 742.
- [18] J. P. Chen, C. M. Sorensen, K. J. Klabunde, G. C. Hadjipanayis, *J. Appl. Phys.* 76 (1994) 6316.
- [19] J. A. L. Perez, M. A. L. Quintela, J. Mira, J. Rivas, S. W. Charles, *J. Phys. Chem. B* 101 (1997) 8045.
- [20] Q. Chen and Z. J. Zhang, *Appl. Phys. Lett.* 73 (1998) 3156.
- [21] J. M. D. Coey, *Can. J. Phys.* 65, 1210, 1987.
- [22] L. Neel, *C.R. Acad. Sci. Paris* 230,375,1950.
- [23] A. Rosencwaig, *Canadian J. Phys.* 48, 2857, 1970.